Journal of Inflammation Research

Dovepress
Taylor & Francis Group

Open Access Full Text Article

ORIGINAL RESEARCH

Role of Aging in Ulcerative Colitis Pathogenesis: A Focus on ETS1 as a Promising Biomarker

Man Ni[1,2], Weilong Peng[1,2], Xiaoguang Wang[1,2], Jingui Li[1,2]

[1]School of Veterinary Medicine, Jiangsu Co-Innovation Center for Prevention and Control of Important Animal Infectious Diseases and Zoonoses, Yangzhou University, Yangzhou, 225009, People's Republic of China; [2]Joint International Research Laboratory of Agriculture and Agri-Product Safety, the Ministry of Education of China, Yangzhou University, Yangzhou, Jiangsu, 225009, People's Republic of China

Correspondence: Jingui Li, School of Veterinary Medicine, Yangzhou University, No. 48, Daxue North Road, Hanjiang District, Yangzhou City, Jiangsu, 225009, People's Republic of China, Email jgli@yzu.edu.cn

Purpose: An increasing proportion of the aging population has led to a rapid increase in the number of elderly patients with ulcerative colitis (UC). However, the molecular mechanisms by which aging causes UC remain unclear. In this study, we explored the role of aging-related genes (ARGs) in UC pathogenesis and diagnosis prediction.

Methods: Gene expression data were obtained from four independent datasets (GSE75214, GSE87466, GSE94648, and GSE169568) in the GEO database, and ARGs were derived from multiple public databases. After identifying UC-related ARGs, consistent clustering was performed to screen aging-related molecular subtypes, followed by the exploration of differences in the immune microenvironment and pathways between distinct subtypes. Next, core module genes were screened using WGCNA and then the hub genes were characterized using LASSO and random forest methods. Besides, the associations between hub genes, immune cells, and key pathways were explored. Finally, the expression levels of key genes were determined in a dextran sulfate sodium (DSS)-induced UC mouse model by qRT-PCR.

Results: UC samples were classified into two subtypes (1 and 2), which displayed significant differences in the immune landscape and JAK/STAT signaling pathways. A series of machine learning algorithms was used to screen two feature genes (ETS1 and IL7R) to establish the diagnostic model, which exhibited satisfactory diagnostic efficiency. In addition, these hub genes were closely associated with the infiltration of specific immune cells (such as neutrophils, memory B cells, and M2 macrophages) as well as with the JAK/STAT pathway. Later, experimental validation confirmed that ETS1 expression was markedly increased in a mouse model of UC.

Conclusion: Overall, aging, immune dysregulation, and UC process are closely associated. The identified feature genes, particularly ETS1, could serve as novel diagnostic biomarkers for UC. These findings have the potential to enhance the understanding of the age-related mechanisms of UC.

Keywords: ulcerative colitis, aging, machine learning, immune microenvironment, biomarker

Introduction

Ulcerative colitis (UC) is a persistent and recurrent inflammatory bowel disease (IBD) in which lesions initiate in the rectum and subsequently spread to the colonic mucosa.[1] It has become a global public health problem that seriously affects patients' quality of life.[2] As the population ages and the prevalence of IBD increases, the number of older patients with UC is on the rise.[3] Approximately 10%-30% of the UC population is reported to be over 60 years of age, including patients with a long-term course and those with older-onset cases (age at diagnosis ≥ 60 years).[4] The clinical management of elderly UC patients is complex, and treatment with surgery or immunomodulators may result in a higher risk of infection and malignancy than in younger adults.[5] Despite the high safety profile of new biologic therapies, such as vedolizumab,[6] clinically available agents for elderly UC patients are still lacking. Hence, an understanding of the pathogenesis of aging-related UC could help to explore new protective drugs, aiming to reduce the impact of this disease on global public health.

Aging is a complex biological phenomenon that involves the progressive loss of the physiological functions of multiple organs.[7] With increasing age, significant structural and functional changes occur in intestinal stem cells,

Received: 31 October 2024
Accepted: 18 January 2025
Published: 6 February 2025

Graphical Abstract

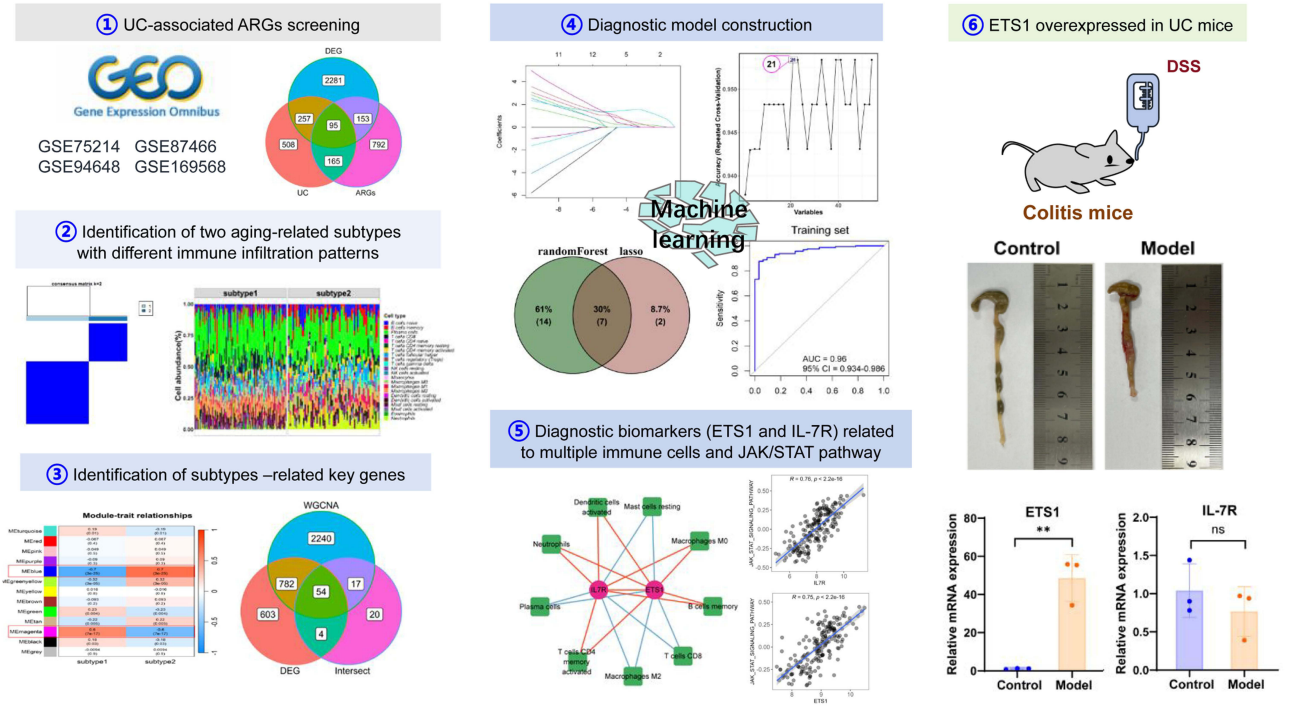

intestinal mucosa, and intestinal microenvironment.[8–10] These cumulative changes cause dysregulation of the intestinal immune system, promoting an increase in the number of immune cells, leading to low levels of chronic inflammation.[11] This persistent inflammation subsequently disrupts the homeostasis of the mucosal microenvironment, which impairs the function of the intestinal epithelium, ultimately contributing to the susceptibility of older adults to gastrointestinal disorders such as UC.[12] Aging-related genes (ARGs) exert critical roles in the onset and regulation of age.[13] Currently, the identification of the key signature of ARGs has been reported to have predictive value in the diagnosis and therapeutic response of gastrointestinal tumors, such as colorectal and gastric cancer.[14,15] However, the exact mechanisms by which aging causes UC have not been explored. Thus, identifying the key ARGs and molecular processes involved in UC may provide a theoretical basis for the diagnosis and prevention of aging-related UC.

In this study, we combined UC gene expression profiles and aging-related databases to determine key ARGs in UC using machine learning algorithms and animal experiments. In addition, a growing body of literature suggests that the JAK/STAT signaling pathway contributes to aging-related systemic inflammation, and its inhibitors are expected to attenuate aging-associated dysfunction.[16] Therefore, we elucidated the association between biomarkers and the JAK/STAT pathway using GSVA. We also revealed the immune mechanisms of UC by immune infiltration analysis. This study was designed to provide insights into the links between aging, immune landscape, and UC.

Materials and Methods

Data Acquisition

Microarray data of four datasets were acquired from the GEO database (http://www.ncbi.nlm.nih.gov/geo/), including GSE75214,[17] GSE87466,[18] GSE94648,[19] and GSE169568.[20] GSE75214 (GPL6244 platform, containing 74 UC and 11 normal samples) and GSE87466 (GPL13158 platform, containing 87 UC and 21 normal samples) were used as the training sets to identify molecular subtypes and diagnostic biomarkers. GSE94648 (GPL19109 platform, including 25 UC and 22 normal samples) and GSE169568 (GPL10558 platform, including 58 UC and 30 normal samples) were used

as validation sets to confirm the diagnostic value of biomarkers. To eliminate the batch effect between different datasets, the sva function in R was used to merge data from GSE75214 and GSE87466.

ARGs were collected from the CellAge (https://genomics.senescence.info/cells/), GenAge (http://genomics.senescence.info/genes), and Aging Atlas (https://bigd.big.ac.cn/aging/index) databases. After integration, 1205 genes were screened for further analysis. In addition, UC-related genes were extracted from three databases (GeneCards [https://www.genecards.org/], DisGeNET [https://disgenet.cn/], and CTD [https://ctdbase.org/]) and ultimately 1025 genes were obtained after integration.

Screening of Differentially Expressed ARGs (DE-ARGs) in UC

Based on the training set data, differential expression analysis of UC and normal samples was conducted using R package limma. Differentially expressed genes (DEGs) were selected using $P < 0.05$ and $|\log_2 FC| > 0.5$ as screening criteria, followed by visualization of the volcano plot and heatmap drawn by R package ggplot2. Next, the overlapping genes associated with ARGs, DEGs, and UC were identified by using R package UpSetR, which were considered as DE-ARGs.

Gene Set Variation Analysis (GSVA)

GAVA is a nonparametric, unsupervised method that can be used to assess changes in the activity of gene sets from different samples.[21] The JAK/STAT signaling pathway is involved in the regulation of inflammatory responses and has been proven to be a valuable target for UC treatment.[22] Here, we observed the enrichment levels of this pathway in normal and UC samples. Briefly, the gene set of the JAK/STAT signaling pathway was downloaded from the MSigDB database (http://www.broadinstitute.org/gsea/msigdb/index.jsp), and enrichment analysis was performed using the R package GSVA to calculate the score of the pathway in the samples. Afterward, the difference in GSVA scores between the two groups were compared using the *t*-test.

Immune Infiltration Assessment

UC-associated inflammatory responses are thought to be caused by immune dysregulation, but this is not yet fully understood. CIBERSORT is a computational method for the quantification of cellular components from large tissue gene expression profiles obtained by RNA sequencing.[23] Hence, we applied the CIBERSORT tool to estimate the proportion of 22 immune cell types in samples from the training set. In addition, under the threshold of $P < 0.05$, differences in the abundance of immune cell infiltration between the UC and normal groups were observed.

ARGs-Associated Subtypes Analysis

Identification of intrinsic subgroups with common biological characteristics is achieved by using the "ConsensusClusterPlus" package in R.[24] To explore the potential subtypes of patients with AA, we employed the ConsensusClusterPlus software to perform cluster analysis of DE-ARGs. The number of clusters k was set from 2 to 10, and the optimal subtypes were recognized based on the cumulative distribution function (CDF). The characteristics of immune infiltration and the JAK/STAT pathway between different subtypes were further analyzed, followed by a comparison of the differences between subtypes using a *t*-test. DEGs in different subtypes were identified using the R package limma with a threshold of $P < 0.05$ and $|\log_2 FC| > 0.5$.

WGCNA

WGCNA can be used to identify highly cooperative gene expression matrices and reveal core genes associated with specific phenotypes such as disease states, providing clues for disease mechanism studies.[25] In this study, a scale-free co-expression network was constructed using the R package "WGCNA" based on the gene expression profiles in the merged dataset (GSE75214 and GSE87466). First, the optimal soft-threshold power was determined based on the scale-free topology criterion and the weighted adjacency matrix was constructed. Subsequently, the matrix was transformed into the topological overlay matrix, and then the modules were constructed based on the hierarchical clustering and dynamic tree-cutting function. The minimum number of genes in each module was set to 25 and the modules were merged with a height cut of 0.4. Afterwards, the correlation between each module and clinical features was calculated, and significant

modules related to ARGs were screened with a threshold of $|R| > 0.5$ and $P < 0.05$. Finally, Characteristic genes in core modules were extracted and then intersected with DE-ARGs and DEGs. Shared genes were served as candidate genes for next analysis.

Screening of UC-Related Feature Genes

Compared to traditional statistical methods, machine learning can better mine high-dimensional, complex structures, and basic medical data to screen for variables that serve important roles in categories.[26] Based on the candidate genes, two machine learning algorithms (LASSO and Random Forest) were employed to collectively identify the UC-related feature genes. LASSO is a valuable choice for various data analyses, owing to its advantages in dimensionality reduction, model interpretability, and feature variable selection.[27] In this study, the glmnet package was employed for the LASSO analysis. Meanwhile, random forest can quantitatively describe the contribution value of features to classification, and it is widely used in the analysis of various feature selections.[28] Therefore, we used the R package randomForest for random forest analysis to filter out unimportant genes. The intersection of genes in the two machine learning algorithms was considered the feature genes for UC. In addition, based on these genes, a UC prediction model was established using a logistic regression algorithm. Its predictive effect was evaluated using the ROC curve in the training and validation sets via pROC package.[29]

Animal Experiments

The UC animal model was established as previously described.[30] First, eight-week-old C57BL/6 male mice (from Medical School Experimental Animal Center of Yangzhou University) were acclimatized for 7 days in a pathogen-specific animal facility with a controlled environment of 40%-70% relative humidity, 18–26°C, and 12/12-h light/dark cycle. Subsequently, based on the method described in the previous article,[30] mice were administered 3% dextran sodium sulfate (DSS, MeilunBio, 9011–18-1) solution (3 g DSS powder dissolved in 100 mL of sterile distilled water) for 7 days to induce colitis. Mice in the control group drank equal amounts of water throughout the experiment. Each group consisted of six animals. During this period, body weight, fecal occult blood, and stool consistency of mice were recorded daily. The sum of the three indicators was defined as the Disease Activity Index (DAI), which was calculated based on grading criteria to assess the severity of intestinal inflammation.[31] The specific scoring rules are as follows: (i) body weight loss: 0 point = none, 1 point = 1–5%, 2 points = 5–10%, 3 points = 10–15%, 4 points = over 15%; (ii) fecal occult blood: 0 point = no blood, 2 points = visual pellet bleeding, 4 points = severe bloody stool and blood around the anus; (iii) stool consistency, 0 point = normal, 2 points = dilute stool, 4 points = diarrhea. Mice were euthanized on day 8 and colon tissues were collected for further study. All experiments adhered to guidelines approved by the Ethical Review Committee for Animal Experiments of Yangzhou University (202411028).

Assessment of Colon Macroscopic Damage Index (CMDI)

We first evaluated histological changes in the colon by measuring its length. In addition, the colon was dissected longitudinally along the mesenteric side on ice and changes in the morphology of the colon were observed visually. The CMDI was used to reflect the severity of ulcer formation and inflammation, and its scoring rules are calculated according to the previous research.[32] The specific scoring rules are as follows: 0 point = no damage, 1 point = mild congestion and edema, smooth surface, without erosion or ulceration, 2 points = hyperemia edema, mucosal roughness, granulation, erosions or intestinal adhesion, 3 points = severe surface congestion and edema, necrosis, ulcer formation, intestinal wall thickening or surface necrosis, inflammatory polyps, 4 points = severe congestion and edema, mucosal necrosis and ulcer formation, total intestinal wall necrosis, toxic megacolon death.

Detection of Key Genes by qRT-PCR

qRT-PCR experiments were conducted as previously described.[33] Total RNA was isolated from the colon tissues using an RNAsimple kit (TIANGEN, DP419). Reverse transcription and amplification reactions were conducted using the FastKing RT kit (TIANGEN, KR118-02) and Taq Pro Universal SYBR qPCR Master Mix (Vazyme, Q712-02) kit, according to the manufacturer's protocol. Finally, the relative expression of each gene was normalized to that of GAPDH, and relative expression

levels were calculated using the $2^{-\Delta\Delta Ct}$ method. The primer sequences used in this study were as follows: Ets-1 (127 bp) forward, 5'-CCAGTCATCCTTCAACAGCC-3' and reverse, 5'-AGCACCGTCACGCACATAGT-3'; IL-7R (126 bp) forward, 5'-GCGGACGATCACTCCTTCTG-3' and reverse, 5'-AGCCCCACATATTTGAAATTCCA-3'; GAPDH (211 bp) forward, 5'-TGGATTTGGACGCATTGGTC-3' and reverse, 5'-TTTGCACTGGTACGTGTTGAT-3'.

Data Statistics

All bioinformatic analyses were implemented using R software (version 4.2.2). Logistic regression analysis was used to determine the diagnostic classification model, followed by evaluation of its predictive performance by plotting ROC curve and calculating the area under the curve. Correlations between biomarkers and immune or the JAK/STAT pathway were assessed by Pearson method. Besides, each experiment was repeated at least three times. All experimental data were expressed as mean ± standard deviation (SD) and were statistically analyzed/visualized by GraphPad Prism (version 8.0). The differences between the two groups were compared using Student's *t*-test (normally distributed data) or Kruskal–Wallis test (non-normally distributed data). $P < 0.05$ was considered statistically significant.

Results

Identification of DEGs in UC Vs Normal Samples

After removing the batch effect, the samples in the two datasets were uniformly dispersed, indicating that reliable results were obtained (Figure 1A). In total, 1025 shared UC-related genes were identified in the three databases (Figure 1B). In addition, Limma was used to characterize DEGs in UC versus normal samples, and 2786 DEGs were screened, with 1624 up-regulated and 1162 down-regulated genes (Figure 1C). The top 30 DEGs (sorted by $|\log_2 FC|$) are displayed in a heatmap (Figure 1D). Subsequently, to explore the significance of aging in UC pathology, we performed Venn analysis to integrate DEGs, UC, and ARGs, and finally determined 95 DE ARGs for further analyses (Figure 1E). In addition, GSVA revealed abnormal activation of the JAK/STAT signaling pathway in UC samples ($P < 0.0001$, Figure 1F). The JAK/STAT signaling pathway plays a crucial role in the regulation of immune and inflammatory responses.[34] The latest study has identified unique inflammation-associated cell state in the epithelium of UC patients, mainly attributed to JAK/STAT pathway activation. This is consistent with our findings.

Analysis of Immune Cell Infiltration in UC and Normal Samples

Considering that UC is characterized by immune disorders, we employed the CIBERSORT algorithm to analyze 22 cell types in samples from the training set. As shown in Figure 2A, plasma cells, M2 macrophages, and resting mast cells accounted for a higher proportion of infiltration in normal and UC samples. Notably, UC and normal samples had distinctly different immune profiles. Fourteen different immune cell types were observed in both the groups (Figure 2B). For example, compared to normal controls, the abundance levels of memory B cells, M1 macrophages, and activated dendritic cells in UC samples were clearly increased, whereas the levels of M2 macrophages and resting mast cells were decreased. The level of these cell infiltrations has been confirmed to be significantly different between UC patients and normal individuals.[35]

Screening of Two Aging-Related Subtypes in UC

To comprehensively understand the expression patterns of ARGs in UC, we used a consensus clustering algorithm based on the expression of 95 DE-ARGs. The CDF curves showed that the curves had a lower slope when k = 2, indicating that the clustering results were reliable (Figure 3A). Thus, the entire cohort was classified into two aging-related subtypes (Figure 3B). PCA further confirmed that the two subtypes could be clearly distinguished (Figure 3C). Next, to investigate the role of ARGs in the immune microenvironment, the infiltration levels of immune cells in the two subtypes were analyzed using the CIBERSORT algorithm. As expected, two subtypes displayed different patterns of immune infiltration. We also observed that plasma cells and M2 macrophages were predominant in both subtypes (Figure 3D). Eleven immune cells exhibited significantly different abundance levels between subtypes 1 and 2 (Figure 3E). Among them, subtype 1 had elevated levels of plasma cells, CD8 T cells, M2 macrophages, and resting mast cells, whereas subtype

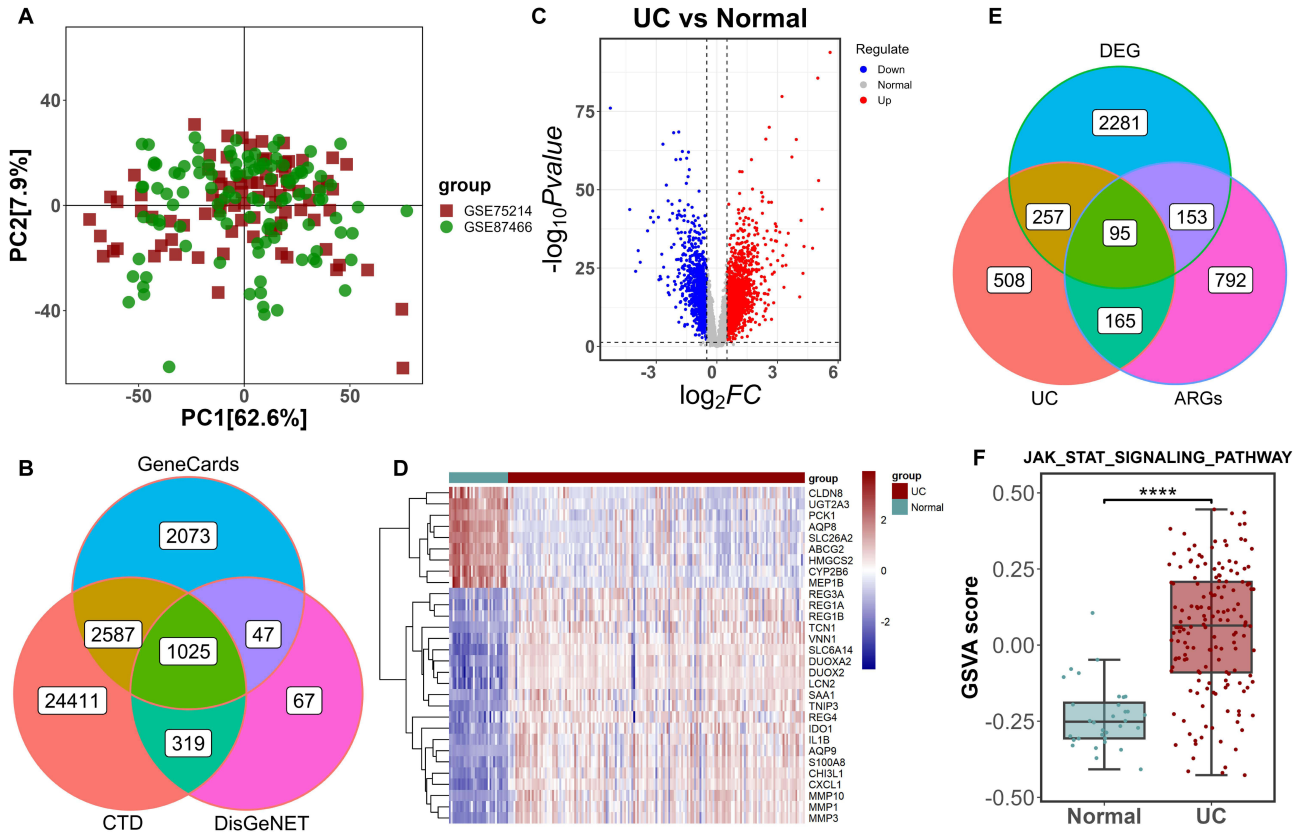

Figure 1 Identification of DE-ARGs in UC and normal samples. (**A**) PCA plot shows the distribution patterns of the samples in the two datasets (GSE75214 and GSE87466) after removing the batch effect. (**B**) Venn diagram shows UC-related genes from three databases (GeneCards, CTD, and DisGeNET). (**C**) Volcano plot of DEGs between UC and normal samples. Blue node represents down-regulated gene, red node represents up-regulated gene, and gray node represents no significant differences. (**D**) Heatmap displays the top 30 DEGs ranked by $|\log_2 FC|$ value. (**E**) Venn diagram of DE-ARGs intersected by UC, DEGs, and ARGs. (**F**) Boxplot of GSVA score for the JAK/STAT signaling pathway in normal and UC groups. JAK/STAT signaling pathway is significantly activated in the UC samples. **** $P < 0.0001$.

Abbreviations: DE-ARGs, differentially expressed aging-related genes; UC, ulcerative colitis; PCA, Principal component analysis; DEGs, differentially expressed genes; ARGs, aging-related genes.

2 had elevated levels of memory B cells, activated dendritic cells, and neutrophils. In addition, GSVA revealed a significant enrichment of the JAK/STAT signaling pathway in subtype 2 (Figure 3F). Furthermore, differential expression analysis identified 1443 DEGs (606 up-regulated and 837 down-regulated) in subtypes 1 and 2. The volcano plot shows the distribution of all DEGs and the heatmap displays the top 30 DEGs (Figure 3G and H).

Identification of Key Modules Through WGCNA

We used WGCNA to identify core modules associated with these subtypes. When the soft threshold was 6, the biological network reached scale-free and the connectivity tended to be smooth; thus, it served as the optimal threshold (Figure 4A). A cluster tree diagram of all the samples is shown in Figure 4B. Thirteen clusters related to subtypes were detected, with the blue and magenta modules having the strongest association with molecular subtypes (Figure 4C). Blue indicates a negative correlation with subtype 1 ($r = -0.7$, $P = 3e\text{-}25$), while magenta indicates a positive correlation with subtype 1 ($r = 0.6$, $P = 7e\text{-}17$). Afterward, The Venn diagram revealed 54 overlapping genes in WGCNA, DEGs in subtypes, and DE-ARGs that were used for subsequent exploration (Figure 4D).

Screening for Diagnostic Biomarkers in UC

With the help of two machine learning algorithms, the characteristic genes in UC were identified. LASSO analysis determined nine key variables, and the gene contraction tended to be stable (Figure 5A and B). The random forest model screened 21 genes, corresponding to the highest accuracy rate (Figure 5C). Figure 5D shows the ranking of important gene contributions in the random forest model based on the MeanDecreaseGini. Seven shared biomarkers (CD34,

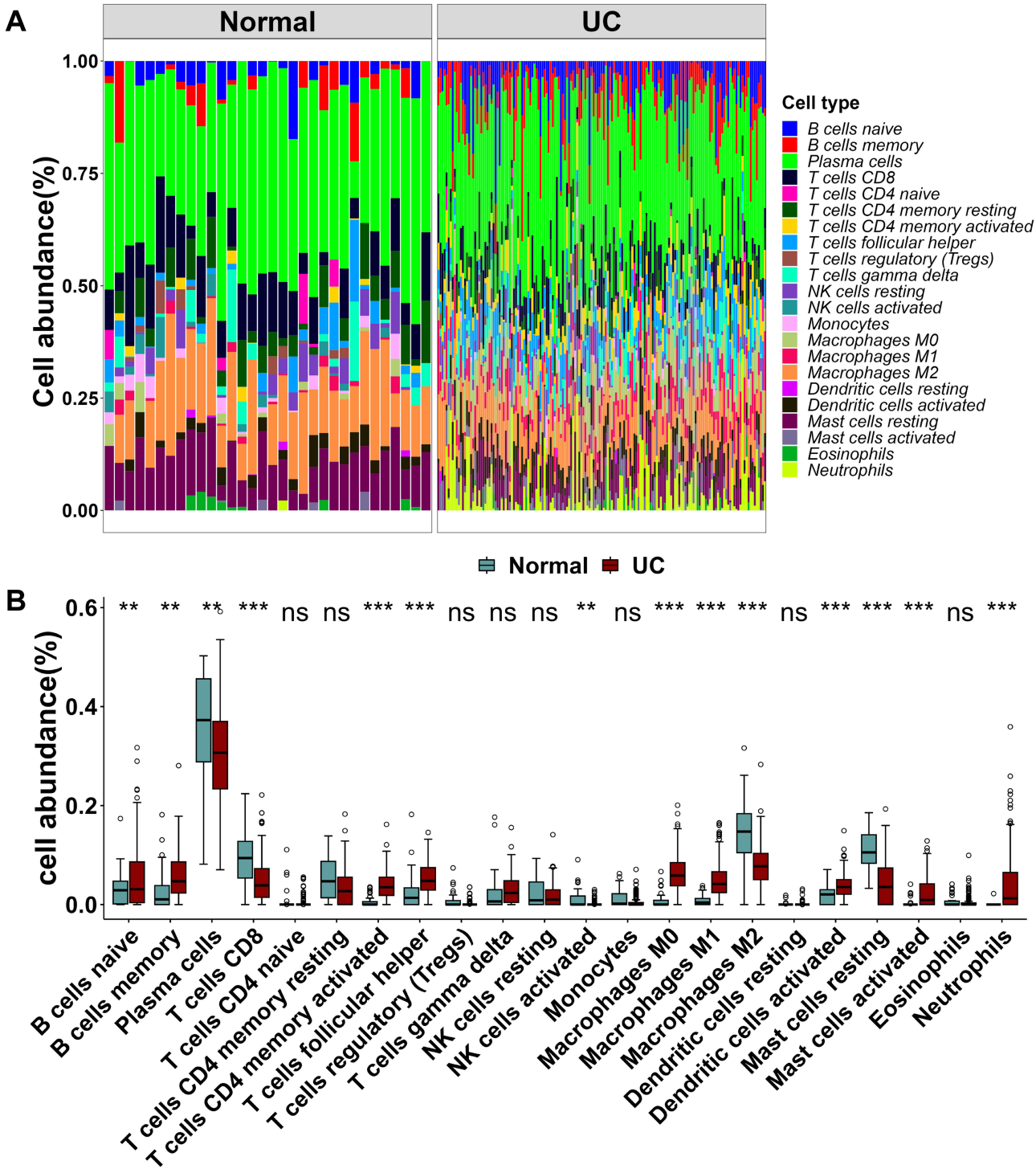

Figure 2 Analysis of immune cell infiltration in the UC and normal samples. (**A**) Bar plot reveals the proportion of 22 immune cells in UC and normal samples. (**B**) Comparison of the abundance level of immune cells in UC and normal samples. Ns, no significant; ** P < 0.01; *** P < 0.001.

CXCL1, ETS1, IL1RN, IL7R, TIMP1, and VCAM1) were identified by integrating these two algorithms (Figure 5E). With the development of complex biological models, the effectiveness of a single biomarker for clinical diagnosis has gradually become limited. Therefore, we established a multivariate logistic regression model based on these seven biomarkers. The model combining the two variables (ETS1 and IL7R) exhibited satisfactory accuracy and was superior to the other combinations. In the training, GSE169568 validation, and GSE94648 validation sets, the AUC values were

https://doi.org/10.2147/JIR.S504040

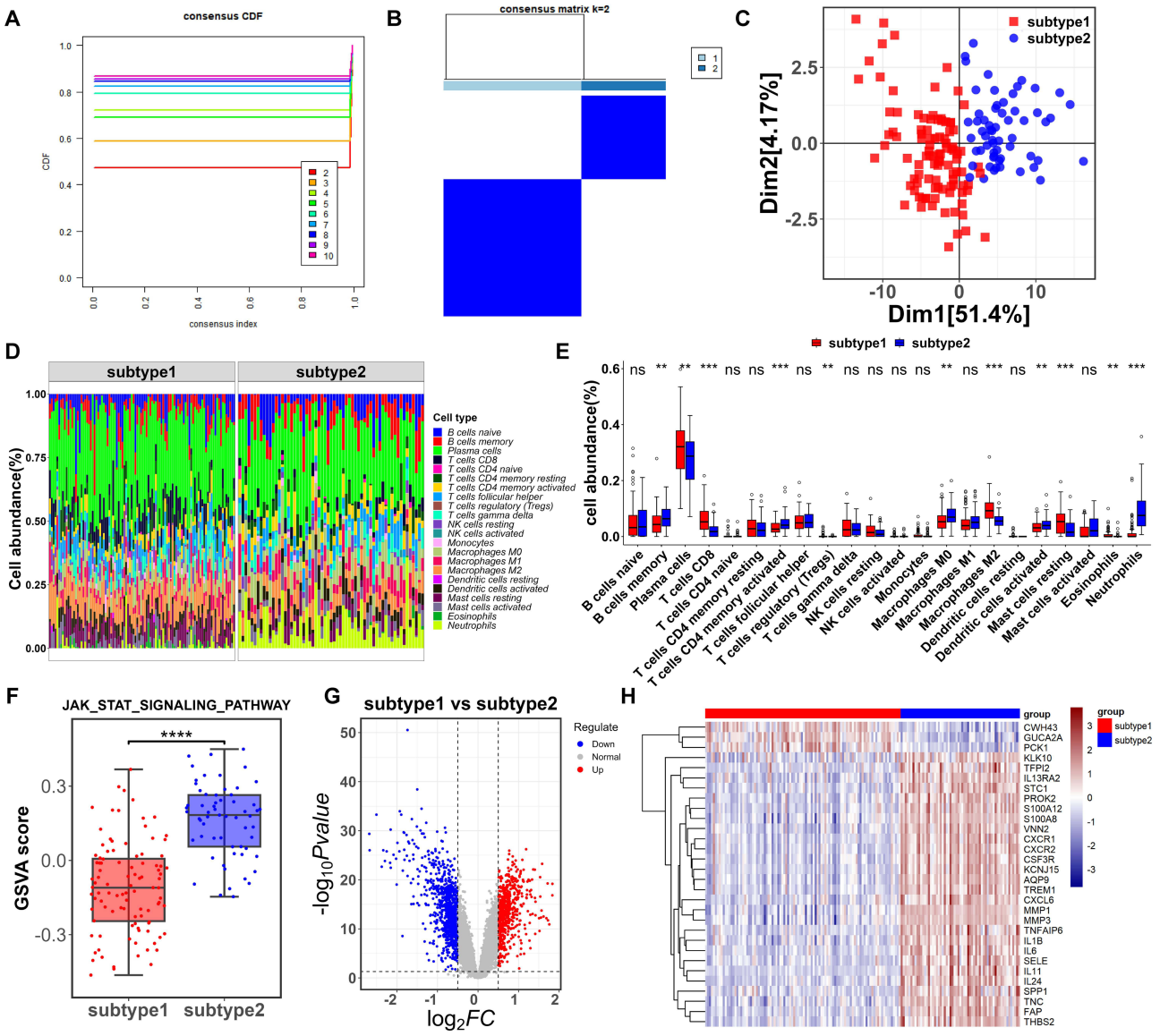

Figure 3 Screening for aging-related subtypes through consensus clustering analysis. (**A**) CDF curves of consensus scores for k = 2–10. When k = 2, the slope of CDF curve is the lowest, indicating that the clustering results are reliable. (**B**) Heatmap of consensus clustering for k = 2. (**C**) PCA plot supports the classification of UC samples into two separate subtypes. (**D**) Bar plot shows the infiltration levels of 22 cells in subtype 1 and subtype 2. (**E**) Comparisons of 22 immune cells infiltration levels between subtype 1 and subtype 2. (**F**) Boxplot of GSVA score for the JAK/STAT signaling pathway in two subtypes. JAK/STAT signaling pathway is significantly activated in the subtype 2 samples. (**G**) Volcano plot of DEGs between subtype 1 and subtype 2. Red dots represent up-regulated genes, blue dots represent down-regulated genes, and gray dots represent no significant differences. (**H**) Heatmap displays the top 30 DEGs in subtype 1 vs subtype 2. Ns, no significant; ** P < 0.01; *** P < 0.001; **** P < 0.0001.
Abbreviation: CDF, Cumulative distribution function.

0.96, 0.817, and 0.882, respectively (Figure 5F and G). An AUC of between 0.8 and 1.0 is considered excellent for the overall diagnostic accuracy of the test.[36] Hence, the model was reliable and accurate for UC diagnosis.

Correlation Analysis of Two Diagnostic Genes and Biological Characteristics

We further observed the link between the genes in the model and differential immune cells or JAK/STAT signaling pathway activity. Results showed that ETS1 and IL7R were positively correlated with activated dendritic cells, neutrophils, activated memory CD4 T cells, memory B cells, and M0 macrophages (red line indicates positive correlation), but negatively associated with resting mast cells, M2 macrophages, and CD8 T cells (blue line indicates negative correlation; Figure 6A). In addition, increased expression of the two diagnostic genes significantly promoted the activity of the JAK/STAT signaling pathway (R = 0.75 for ETS1, R = 0.76 for IL7R; $P < 005$; Figure 6B and C). Taken together,

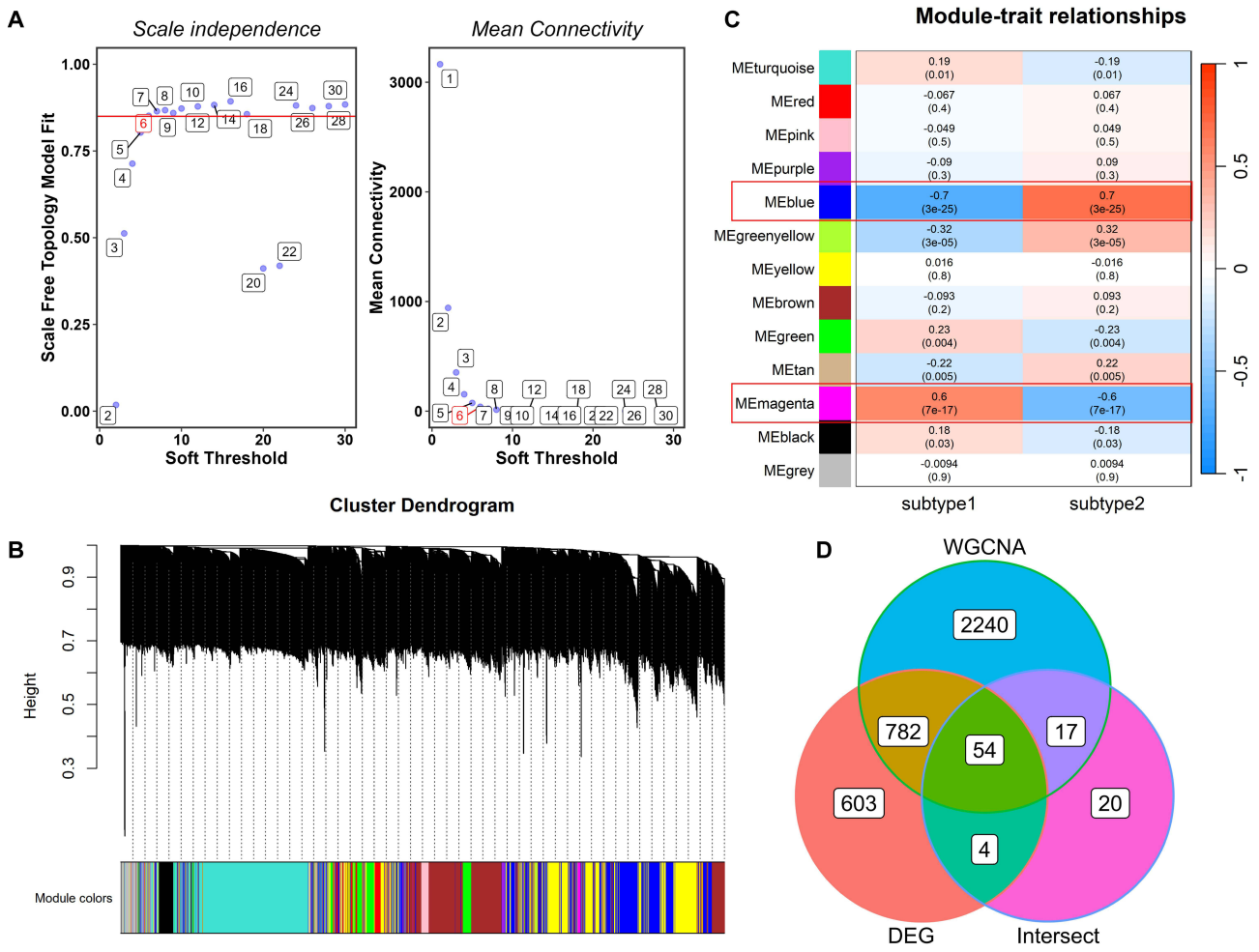

Figure 4 Weighted gene co-expression network analysis (WGCNA). (**A**) Determination of soft threshold power for scale-free topology. A soft threshold of β = 6 ensures that the network achieves scale-free. (**B**) Cluster tree of highly connected genes in modules. Different colors indicate different gene clusters, and gray modules represent genes not attributed to any module. (**C**) Heatmap reveals the relationship between modules and two subtypes. Each cell contains r and P value. Genes in the blue and magenta modules are selected for further analyses. (**D**) Venn diagram of candidate genes intersected by WGCNA, DEGs in subtypes, and DE-ARGs (Intersect).

these two biomarkers may play a role in UC pathogenesis by modulating immune cell infiltration and regulating the JAK/STAT signaling pathway, thereby affecting the inflammatory response in the colon.[37]

Confirmation of Hub Gene Expression Levels in the Experimental Colitis

To confirm the results of the bioinformatic analysis, we established a DSS-induced UC model in mice. Compared to the control group, the body weight of mice in the model group decreased significantly with increasing treatment time (Figure 7A). During this period, the DAI scores of mice in the model group were consistently elevated (Figure 7B). We also observed that the mice administered DSS solution began to show characteristics such as depression, dark fur, and persistent diarrhea on day 4. In addition, bleeding and soft stools were observed around the anus of model mice on day 7 (Figure 7C). Further evaluation showed that the colon length of mice in the model group was obviously shortened and the intestinal mucosa exhibited erosion, congestion, and edema (Figure 7D and E). Meanwhile, the CMDI score of mice in the model group was significantly higher than that of mice in the control group (Figure 7E). These changes intuitively indicated the development of UC in mice, demonstrating that the UC model was successfully constructed.[38] The expression levels of these two genes were determined by qRT-PCR. The results showed that the mRNA level of ETS1 was markedly increased in the model group than in the control group. Although IL-7R expression tended to decline in the model group, it was not significantly associated with UC occurrence (Figure 7F).

https://doi.org/10.2147/JIR.S504040

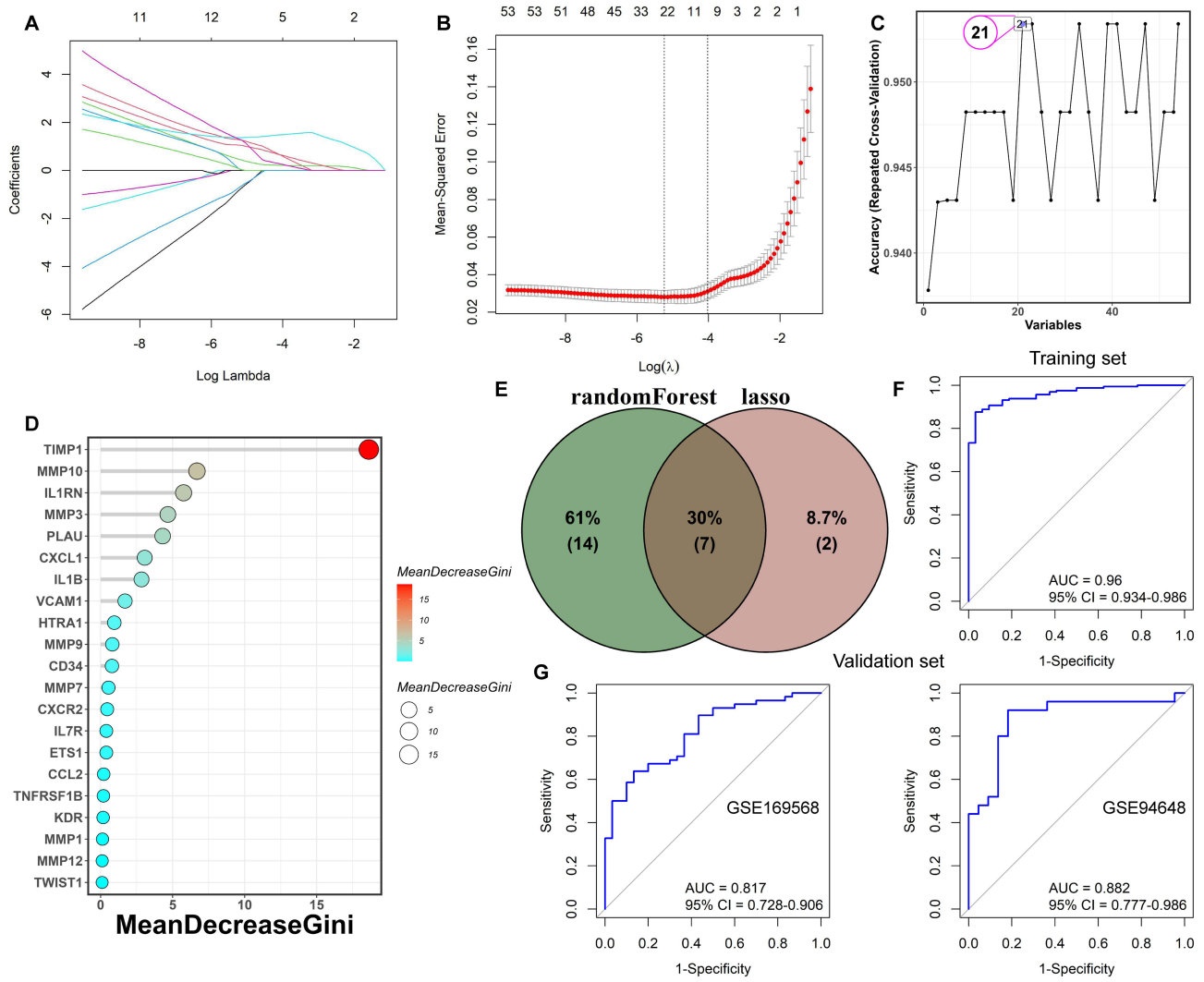

Figure 5 Screening for diagnostic biomarkers in UC through machine learning algorithms. (**A and B**) LASSO model identified the core feature genes in UC. λ = 9 is the optimal parameter. (**C**) Random forest determines the number of variables corresponding the correct rate. When the number of variables is 22, the accuracy of the model is the highest. (**D**) Genes identified by random forest are ranked based on the MeanDecreaseGini score. Higher MeanDecreaseGini values correspond to higher significance of the variable. (**E**) Venn diagram exhibits the seven overlapping genes identified in LASSO and random forest. (**F and G**) The variables screened by Logistic analysis were used to construct the diagnostic model, and finally two genes (ETS1 and IL7R) were included. ROC curves of diagnostic model in training (merged dataset) and validation sets (GSE169568, GSE94648).

Discussion

UC is often refractory, mainly due to the lack of specific drugs and treatments.[39] Moreover, the clinical manifestations of UC are diverse and easily misdiagnosed, and a low diagnostic rate causes a delay in the initial remission of the disease; therefore, early detection remains a daunting task.[40] Therefore, discovery of specific biomarkers that can accurately identify UC is a promising research direction. Currently, the aging population poses unique challenges in the clinical management of UC.[41] Although age is an important factor in UC pathology,[42] a diagnostic model of UC based on ARGs has not yet been developed. In this study, two aging-related subtypes were screened. Seven candidate biomarkers were screened through WGCNA and ARG-based machine learning algorithms. Logistic regression ultimately determined that the model established using the two genes (ETS1 and IL7R) had an accurate predictive value for UC diagnosis. In addition, we observed a direct association between ETS1 and IL7R, immune cell infiltration, and JAK/STAT pathway. Further experiments confirmed that ETS1 was highly expressed in UC mice. These findings may provide novel insights into the treatment of elderly UC patients.

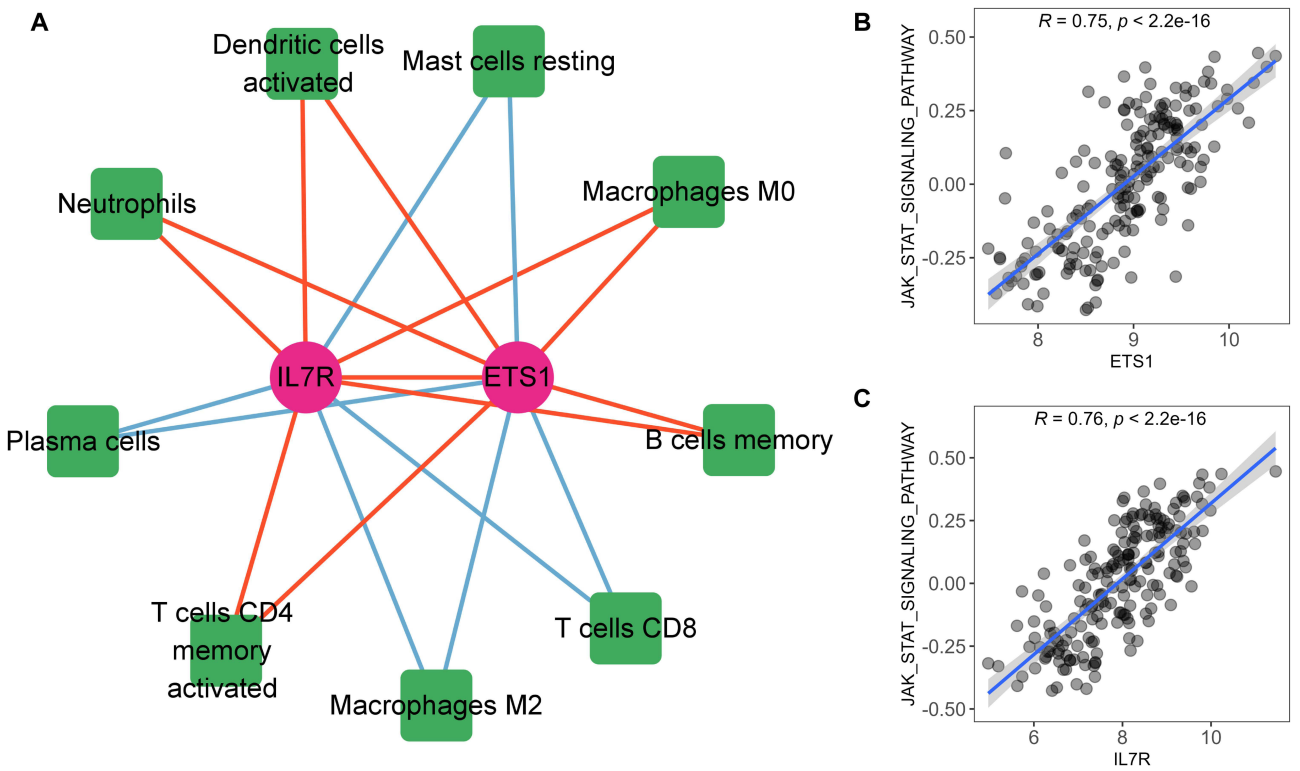

Figure 6 Pearson correlation analysis of two diagnostic genes and biological characteristics. (**A**) Correlation network of key genes (ETS1 and IL7R) and differential immune cells. Red line indicates a positive correlation and blue line indicates a negative correlation. (**B and C**) Scatter plots show positive correlations between ETS1 or IL7R and JAK/STAT signaling pathway.

ETS1 belongs to the ETS family of transcription factors and exerts multiple effects on aging, inflammation, and cancer development.[43,44] Clinical studies have found that inflammatory cytokines such as TNF-α and IL-1β induce the expression and nuclear translocation of epithelial-specific ETS1, thereby promoting apoptosis of colon cells and triggering the development of colon cancer.[45] Similarly, under the stimulation of chronic inflammation, upregulation of ETS1 expression in UC causes apoptosis in small intestinal epithelial cells, which disrupts intestinal epithelial homeostasis and drives UC progression.[46] We also observed that ETS1 was overexpressed in UC samples. The protein encoded by IL7R is a receptor for interleukin 7 and has been found to play a harmful role in immune cell-mediated IBD.[47] Dysregulation of the IL7R pathway in patients with severe IBD has been shown to facilitate the maintenance of chronic inflammation, and IL7R signaling pathway-related gene signatures are predictive biomarkers in patients with refractory UC.[48,49] In addition, blockade of IL7R is effective in restoring intestinal homeostasis, showing therapeutic potential in preclinical animals and in vitro IBD models.[50] Inhibition of IL7R signaling can also exert a therapeutic effect on UC by regulating the homeostasis of effector memory Th7 cells.[51] These evidences further support the critical role of ETS1 and IL7R in the pathogenesis and treatment of UC. However, the specific mechanism of action needs to be further explored.

In immunomodulation, we found that the two diagnostic biomarkers were positively associated with neutrophils and memory B cells while negatively associated with M2 macrophages. In UC pathology, neutrophils release large amounts of reactive oxygen species by infiltrating the colonic mucosa, which directly leads to tissue damage, aggravates intestinal inflammation, and promotes impaired intestinal barrier defense by generating neutrophil extracellular traps (NETs).[52,53] Mechanistically, upon stimulation of inflammatory gut chemokines such as CXCL8, CXCR1/2 expressing neutrophils are recruited to the gut and activate the release of NETs, thereby promoting downstream pathways of epithelial injury and amplifying the inflammatory response.[54] Hence, UC is generally accompanied by higher neutrophil recruitment, consistent with our findings. Dysregulation of memory B cells is associated with pathogenesis of several inflammatory diseases in humans. In the pathogenesis of UC in animals or patients, the number of (CD27+) (CD19+) (IgG+) memory B cells in the peripheral blood is distinctly reduced, and astragalus polysaccharide treatment can improve UC by restoring the balance of

https://doi.org/10.2147/JIR.S504040

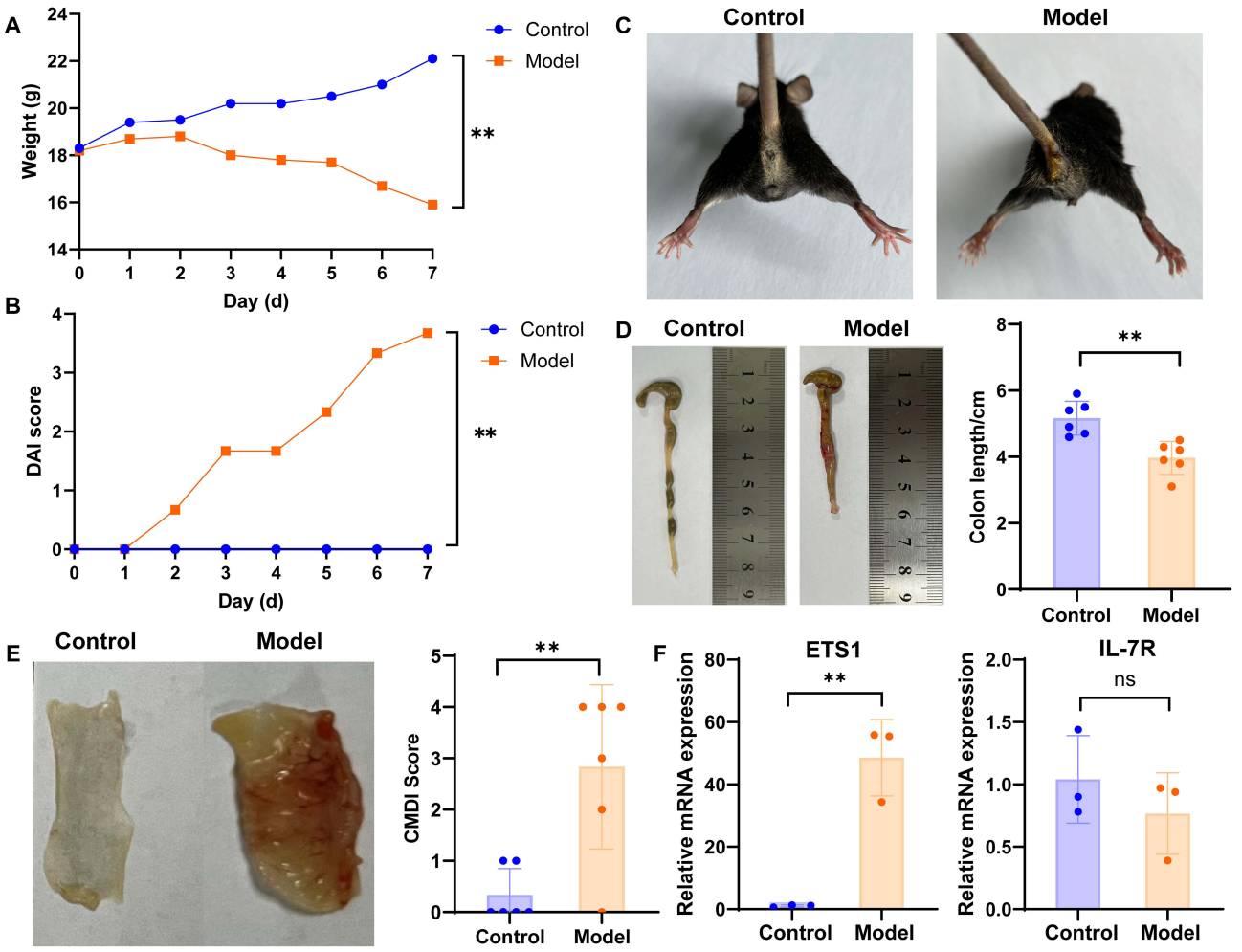

Figure 7 The expression of feature genes in the mouse model of UC. Mice in each group were given water (Control) or 3% DSS (Model) for 7 days. During this period, the body weight, fecal occult blood, and stool consistency of the mice were recorded daily. On day 8, the mice were euthanized and colon tissues were collected. (**A and B**) Body weight and DAI score of mice after DSS treatment. (**C**) Anal bleeding status in mice. (**D**) Representative intestinal tissue image and colon length of mice. (**E**) Colonic mucosal injury index. (**F**) The mRNA expression of ETS1 and IL7R in colon tissue detected by qRT-PCR. ** $P < 0.01$ vs control group.

memory B cells.[55,56] However, in this study, the abundance of memory B cells increased in UC samples, which is inconsistent with previous findings. This may be due to the fact that memory B cells are phenotypically diverse, with functional differences.[57] Future characterization of memory B cell subtypes in UC, using single-cell sequencing, will explain our findings. M2 macrophages contribute to the maintenance of intestinal homeostasis and exhibit anti-inflammatory properties.[55] The decrease in M2 macrophages in UC patients causes the release of pro-inflammatory molecules, leading to the disruption of tight junction proteins and exacerbating of disease progression.[58] Besides, decreased M2 macrophages can impede mucosal healing in UC.[59] Taken together, we speculate that ARGs may promote UC by regulating homeostasis between the inflammatory environment and immune cells; however, the specific mechanism needs to be further explored.

We also observed a positive correlation between ETS1 and IL7R, and the JAK/STAT pathway. This pathway is involved in a variety of cellular processes such as cell division/death and immune regulation, and its overactivation has been associated with inflammatory diseases.[60] Previous study has indicated that blocking JAK mediated inflammatory pathways can alter the innate and adaptive immune responses involved in IBD, thereby reducing chronic gastrointestinal inflammation.[61] JAK/STAT is an important pathway in the aging process and serves as a predictive biomarker of frailty (a syndrome in older people).[62] Targeting this pathway is expected to be an alternative approach for ameliorating age-related dysfunction.[16] Taken together, these findings suggest the possibility of targeting this pathway as a therapeutic option for age-related UC.

For the first time, we constructed a novel UC prediction model based on ARGs and explored their characteristic genes and immune landscapes. Although we utilized a large sample dataset and animal experiments to improve the reliability of our results, it is important to acknowledge that this study had some limitations. First, there is a lack of clinical information for the sample in the GEO database; therefore, direct clinical evidence of the potential effects of age on UC is unavailable. We only performed a simple expression validation in a mouse model, and the detailed mechanisms of how ETS1 or IL7R affect immune response and inflammation, leading to UC pathological processes, are unclear. Further experimental studies are required to improve the credibility of our results.

Conclusion

In this study, the important role of aging in UC was confirmed by integrating bioinformatics analysis, machine learning algorithms, and in vivo experimental validation. Two age-related molecular subtypes with different immune infiltration patterns were identified in UC. DEGs between two subtypes might affect the immune microenvironment of UC by regulating the JAK/STAT signaling pathway. Notably, two machine learning methods and logistic regression screened two key ARGs (EST1 and IL7R) to establish a diagnostic model for accurate prediction of the risk of UC occurrence. We found complex interactions between the two biomarkers and multiple immune cells, including neutrophils, memory B cells, and M2 macrophages. Besides, two genes were positively associated with the JAK/STAT signaling pathway. Afterwards, preliminary experiments revealed that ETS1 was significantly up-regulated in DSS-induced UC mice. Overall, these findings provide important information for the development and application of anti-aging target drugs in UC therapy.

Data Sharing Statement

Publicly available datasets were analyzed in this study. These data can be found from GEO database (http://www.ncbi.nlm.nih.gov/geo/), with the following accession numbers: GSE75214, GSE87466, GSE94648, and GSE169568. The original data from the experiments are available upon reasonable request. Further inquiries can be directed to the corresponding authors.

Ethics Approval and Consent to Participate

In accordance with national legislative guidelines on human data, our research does not require approval, is derived from Article 32, items (1) and (2) of the "Measures for the Ethical Review of Life Science and Medical Research Involving Human Subjects" issued by China on February 18, 2023. The legislation in these two items is that research using legally obtained public data, data generated through observation without interfering with public behavior, or research using anonymized information data can be exempted from ethical approval. This study complied with the Declaration of Helsinki and was approved by the Ethical Review Committee for Animal Experiments of the Yangzhou University (202411028).

Author Contributions

All authors made a significant contribution to the work reported, whether in the conception, study design, execution, acquisition of data, analysis, and interpretation, or in all these areas, took part in drafting, revising, or critically reviewing the article; gave final approval of the version to be published; have agreed on the journal to which the article has been submitted; and agree to be accountable for all aspects of the work.

Funding

This work was supported by the National Natural Science Foundation of China [grant numbers 32473077].

Disclosure

The authors declare no competing interests in this work.

References

1. Kobayashi T, Siegmund B, Le Berre C, et al. Ulcerative colitis. *Nature Reviews Disease Primers*. 2020;6(1):74. doi:10.1038/s41572-020-0205-x
2. Segal JP, LeBlanc J-F, Hart AL. Ulcerative colitis: an update. *Clin Med*. 2021;21(2):135–139. doi:10.7861/clinmed.2021-0080
3. Jeuring SFG, van den Heuvel TRA, Zeegers MP, et al. Epidemiology and long-term outcome of inflammatory bowel disease diagnosed at elderly age-an increasing distinct entity? *Inflamm Bowel Dis*. 2016;22(6):1425–1434. doi:10.1097/MIB.0000000000000738
4. Shrestha MP, Taleban S. Management of ulcerative colitis in the elderly. *Drugs Aging*. 2019;36(1):13–27. doi:10.1007/s40266-018-0611-x
5. Hong SJ, Katz S. The elderly IBD patient in the modern era: changing paradigms in risk stratification and therapeutic management. *Ther Adv Gastroenterol*. 2021;14:17562848211023399. doi:10.1177/17562848211023399
6. Shashi P, Gopalakrishnan D, Parikh MP, et al. Efficacy and safety of vedolizumab in elderly patients with inflammatory bowel disease: a matched case-control study. *Gastroenterol Rep*. 2020;8(4):306–311. doi:10.1093/gastro/goz041
7. Cai Y, Song W, Li J, et al. The landscape of aging. *Sci China Life Sci*. 2022;65(12):2354–2454. doi:10.1007/s11427-022-2161-3
8. Brunet A, Goodell MA, Rando TA. Ageing and rejuvenation of tissue stem cells and their niches. *Nat Rev mol Cell Biol*. 2023;24(1):45–62. doi:10.1038/s41580-022-00510-w
9. Choi J, Houston M, Wang R, et al. Intestinal stem cell aging at single-cell resolution: transcriptional perturbations alter cell developmental trajectory reversed by gerotherapeutics. *Aging Cell*. 2023;22(5):e13802. doi:10.1111/acel.13802
10. Thevaranjan N, Puchta A, Schulz C, et al. Age-associated microbial dysbiosis promotes intestinal permeability, systemic inflammation, and macrophage dysfunction. *Cell Host Microbe*. 2017;21(4):455–466.e4. doi:10.1016/j.chom.2017.03.002
11. Soenen S, Rayner CK, Jones KL, et al. The ageing gastrointestinal tract. *Curr Opin Clin Nutr Metab Care*. 2016;19(1):12–18. doi:10.1097/MCO.0000000000000238
12. Choi J, Augenlicht LH. Intestinal stem cells: guardians of homeostasis in health and aging amid environmental challenges. *Exp. Mol. Med.* 2024;56(3):495–500. doi:10.1038/s12276-024-01179-1
13. Song Q, Hou Y, Zhang Y, et al. Integrated multi-omics approach revealed cellular senescence landscape. *Nucleic Acids Res*. 2022;50(19):10947–10963. doi:10.1093/nar/gkac885
14. Yue T, Chen S, Zhu J, et al. The aging-related risk signature in colorectal cancer. *Aging*. 2021;13(5):7330–7349. doi:10.18632/aging.202589
15. Zhang Y, Yan Y, Ning N, et al. A signature of 24 aging-related gene pairs predict overall survival in gastric cancer. *Biomed. Eng. Online*. 2021;20(1):35. doi:10.1186/s12938-021-00871-x
16. Xu M, Tchkonia T, Ding H, et al. JAK inhibition alleviates the cellular senescence-associated secretory phenotype and frailty in old age. *Proc Natl Acad Sci USA*. 2015;112(46):E6301–E6310. doi:10.1073/pnas.1515386112
17. Vancamelbeke M, Vanuytsel T, Farré R, et al. Genetic and transcriptomic bases of intestinal epithelial barrier dysfunction in inflammatory bowel disease. *Inflamm Bowel Dis*. 2017;23(10):1718–1729. doi:10.1097/MIB.0000000000001246
18. Li K, Strauss R, Ouahed J, et al. Molecular comparison of adult and pediatric ulcerative colitis indicates broad similarity of molecular pathways in disease tissue. *J Pediatr Gastroenterol Nutr*. 2018;67(1):45–52. doi:10.1097/MPG.0000000000001898
19. Planell N, Masamunt MC, Leal RF, et al. Usefulness of transcriptional blood biomarkers as a non-invasive surrogate marker of mucosal healing and endoscopic response in ulcerative colitis. *J Crohn's Colitis*. 2017;11(11):1335–1346. doi:10.1093/ecco-jcc/jjx091
20. Juzenas S, Hübenthal M, Lindqvist CM, et al. Detailed transcriptional landscape of peripheral blood points to increased neutrophil activation in treatment-naïve inflammatory bowel disease. *J Crohn's Colitis*. 2022;16(7):1097–1109. doi:10.1093/ecco-jcc/jjac003
21. Hänzelmann S, Castelo R, Guinney J. GSVA: gene set variation analysis for microarray and RNA-seq data. *BMC Bioinf*. 2013;14(1):7. doi:10.1186/1471-2105-14-7
22. Cordes F, Foell D, Ding JN, et al. Differential regulation of JAK/STAT-signaling in patients with ulcerative colitis and Crohn's disease. *World J Gastroenterol*. 2020;26(28):4055–4075. doi:10.3748/wjg.v26.i28.4055
23. Newman AM, Liu CL, Green MR, et al. Robust enumeration of cell subsets from tissue expression profiles. *Nature Methods*. 2015;12(5):453–457 doi:10.1038/nmeth.3337.
24. Wilkerson MD, Hayes DN. ConsensusClusterPlus: a class discovery tool with confidence assessments and item tracking. *Bioinformatics*. 2010;26(12):1572–1573. doi:10.1093/bioinformatics/btq170
25. Langfelder P, Horvath S. WGCNA: an R package for weighted correlation network analysis. *BMC Bioinf*. 2008;9(1):559. doi:10.1186/1471-2105-9-559
26. Wang Y, Huang J, Zhang J, Wang F, Tang X. Identifying biomarkers associated with the diagnosis of ulcerative colitis via bioinformatics and machine learning. *Mathematical Biosci Engg*. 2023;20(6):10741–10756. doi:10.3934/mbe.2023476
27. Tibshirani R. The lasso method for variable selection in the Cox model. *Stat Med*. 1997;16(4):385–395. doi:10.1002/(sici)1097-0258(19970228)16:4<385::aid-sim380>3.0.co;2-3
28. Acharjee A, Larkman J, Xu Y, et al. A random forest based biomarker discovery and power analysis framework for diagnostics research. *BMC Med. Genomics*. 2020;13(1):178. doi:10.1186/s12920-020-00826-6
29. Robin X, Turck N, Hainard A, et al. pROC: an open-source package for R and S+ to analyze and compare ROC curves. *BMC Bioinf*. 2011;12(1):77. doi:10.1186/1471-2105-12-77
30. Wu H, Chen Q-Y, Wang W-Z, et al. Compound sophorae decoction enhance s intestinal barrier function of dextran sodium sulfate induced colitis via regulating notch signaling pathway in mice. *Biomed. Pharmacother.* 2021;133:110937. doi:10.1016/j.biopha.2020.110937
31. Kim JJ, Hajib MS, Manocha MM, Khan WI. Investigating intestinal inflammation in DSS-induced model of IBD. *J Visualized Exp*. 2012;(60):3678. doi:10.3791/3678
32. Yang H-J, Jeong SJ, Ryu MS, et al. Protective effect of traditional Korean fermented soybean foods (doenjang) on a dextran sulfate sodium-induced colitis mouse model. *Food Funct*. 2022;13(16):8616–8626. doi:10.1039/d2fo01347a
33. Yuan Y, Li N, Fu M, et al. Identification of critical modules and biomarkers of ulcerative colitis by using WGCNA. *J Inflamm Res*. 2023;16:1611–1628. doi:10.2147/JIR.S402715
34. Xin P, Xu X, Deng C, et al. The role of JAK/STAT signaling pathway and its inhibitors in diseases. *Int Immunopharmacol*. 2020;80:106210. doi:10.1016/j.intimp.2020.106210
35. Lu J, Wang Z, Maimaiti M, et al. Identification of diagnostic signatures in ulcerative colitis patients via bioinformatic analysis integrated with machine learning. *Human Cell*. 2022;35(1):179–188. doi:10.1007/s13577-021-00641-w

36. Mandrekar JN. Receiver operating characteristic curve in diagnostic test assessment. *J Thorac Oncol*. 2010;5(9):1315–1316. doi:10.1097/JTO.0b013e3181ec173d
37. Danese S, Argollo M, Le Berre C, et al. JAK selectivity for inflammatory bowel disease treatment: does it clinically matter? *Gut*. 2019;68(10):1893–1899. doi:10.1136/gutjnl-2019-318448
38. Zhou Y, Ji G, Yang X, et al. Behavioral abnormalities in C57BL/6 mice with chronic ulcerative colitis induced by DSS. *BMC Gastroenterol*. 2023;23(1):84. doi:10.1186/s12876-023-02718-2
39. Bhattacharya A, Osterman MT. Biologic therapy for ulcerative colitis. *Gastroenterol Clin North Am*. 2020;49(4):717–729. doi:10.1016/j.gtc.2020.08.002
40. Murphy ME, Bhattacharya S, Axelrad JE. Diagnosis and monitoring of ulcerative colitis. *Clinics in Colon and Rectal Surg*. 2022;35(6):421–427. doi:10.1055/s-0042-1758047
41. Windsor JW, Kaplan GG. Evolving Epidemiology of IBD. *Current Gastroenterol Reports*. 2019;21(8):40. doi:10.1007/s11894-019-0705-6
42. Tran V, Limketkai BN, Sauk JS. IBD in the elderly: management challenges and therapeutic considerations. *Current Gastroenterol Reports*. 2019;21(11):60. doi:10.1007/s11894-019-0720-7
43. Nakayama T, Ito M, Ohtsuru A, et al. Expression of the ets-1 proto-oncogene in human thyroid tumor. *Modern Pathol*. 1999;12(1):61–68.
44. Wernert N, Justen H-P, Rothe M, et al. The Ets 1 transcription factor is upregulated during inflammatory angiogenesis in rheumatoid arthritis. *J Mol Med*. 2002;80(4):258–266. doi:10.1007/s00109-001-0316-0
45. Lee S-H, Bahn JH, Choi CK, et al. ESE-1/EGR-1 pathway plays a role in tolfenamic acid-induced apoptosis in colorectal cancer cells. *mol Cancer Ther*. 2008;7(12):3739–3750. doi:10.1158/1535-7163.MCT-08-0548
46. Li L, Miao X, Ni R, et al. Epithelial-specific ETS-1 (ESE1/ELF3) regulates apoptosis of intestinal epithelial cells in ulcerative colitis via accelerating NF-κB activation. *Immunol Res*. 2015;62(2):198–212. doi:10.1007/s12026-015-8651-3
47. Willis CR, Seamons A, Maxwell J, et al. Interleukin-7 receptor blockade suppresses adaptive and innate inflammatory responses in experimental colitis. *J Inflamm*. 2012;9(1):39. doi:10.1186/1476-9255-9-39
48. Toedter G, Li K, Marano C, et al. Gene expression profiling and response signatures associated with differential responses to infliximab treatment in ulcerative colitis. *Am J Gastroenterol*. 2011;106(7):1272–1280. doi:10.1038/ajg.2011.83
49. Totsuka T, Kanai T, Nemoto Y, et al. IL-7 Is essential for the development and the persistence of chronic colitis. *J Iimmunol*. 2007;178(8):4737–4748. doi:10.4049/jimmunol.178.8.4737
50. Belarif L, Danger R, Kermarrec L, et al. IL-7 receptor influences anti-TNF responsiveness and T cell gut homing in inflammatory bowel disease. *J Clin Invest*. 2019;129(5):1910–1925. doi:10.1172/JCI121668
51. Song L, Deng Y, Huang J, et al. Effect of curcumin regulated memory Th7 cells in mice with DSS-induced colitis. *Int Immunopharmacol*. 2025;145:113770. doi:10.1016/j.intimp.2024.113770
52. Drury B, Hardisty G, Gray RD, et al. Neutrophil extracellular traps in inflammatory bowel disease: pathogenic mechanisms and clinical translation. *CMGH*. 2021;12(1):321–333. doi:10.1016/j.jcmgh.2021.03.002
53. Biasi F, Leonarduzzi G, Oteiza PI, et al. Inflammatory bowel disease: mechanisms, redox considerations, and therapeutic targets. *Antioxid. Redox Signaling*. 2013;19(14):1711–1747. doi:10.1089/ars.2012.4530
54. Xv Y, Feng Y, Lin J. CXCR1 and CXCR2 are potential neutrophil extracellular trap-related treatment targets in ulcerative colitis: insights from Mendelian randomization, colocalization and transcriptomic analysis. *Front Immunol*. 2024;15:1425363. doi:10.3389/fimmu.2024.1425363
55. Song G, Peng G, Zhang J, et al. Uncovering the potential role of oxidative stress in the development of periodontitis and establishing a stable diagnostic model via combining single-cell and machine learning analysis. *Front Immunol*. 2023;14:1181467. doi:10.3389/fimmu.2023.1181467
56. Wang X, Jiang Y, Zhu Y, et al. Circulating memory B cells and plasmablasts are associated with the levels of serum immunoglobulin in patients with ulcerative colitis. *J Cell & Mol Med*. 2016;20(5):804–814. doi:10.1111/jcmm.12728
57. Kurosaki T, Kometani K, Ise W. Memory B cells. *Nat Rev Immunol*. 2015;15(3):149–159. doi:10.1038/nri3802
58. Dharmasiri S, Garrido-Martin EM, Harris RJ, et al. Human intestinal macrophages are involved in the pathology of both ulcerative colitis and Crohn Disease. *Inflamm Bowel Dis*. 2021;27(10):1641–1652. doi:10.1093/ibd/izab029
59. Deng F, Yan J, Lu J, et al. M2 macrophage-derived exosomal miR-590-3p attenuates DSS-induced mucosal damage and promotes epithelial repair via the LATS1/YAP/ β-catenin signalling axis. *J Crohn's Colitis*. 2021;15(4):665–677. doi:10.1093/ecco-jcc/jjaa214
60. Luo Y, Alexander M, Gadina M, et al. JAK-STAT signaling in human disease: from genetic syndromes to clinical inhibition. *J Allergy Clin Immunol*. 2021;148(4):911–925. doi:10.1016/j.jaci.2021.08.004
61. Harris C, Cummings JRF. JAK1 inhibition and inflammatory bowel disease. *Rheumatology*. 2021;60(Supple 2):ii45–ii51. doi:10.1093/rheumatology/keaa896
62. Samson LD, Engelfriet P, Verschuren WMM, et al. Impaired JAK-STAT pathway signaling in leukocytes of the frail elderly. *Immunity & Ageing: I & A*. 2022;19(1):5. doi:10.1186/s12979-021-00261-w